

# INITIAL APPLICATION OF THE ADAPTIVE GRID AIR QUALITY MODEL

M. Talat Odman, Maudood Khan, Ravi Srivastava, and D. Scott McRae\*

## 1. INTRODUCTION

Grid size (or resolution), when inadequate, can be an important source of uncertainty for air quality model (AQM) simulations. Coarse grids used because of computational limitations may artificially diffuse the emissions, leading to significant errors in the concentrations of pollutant species, especially those that are formed via non-linear chemical reactions. Further, coarse grids may result in large numerical errors. To address this issue, multi-scale modeling and grid nesting techniques have been developed (Odman and Russell, 1991; Odman et al., 1997). These techniques use finer grids in areas that are presumed to be of interest (e.g., cities) and coarser grids elsewhere (e.g., rural locations). Limitations include loss in accuracy due to grid interface problems and inability to adjust to dynamic changes in resolution requirements. Adaptive grids are not subject to such limitations and do not require *a priori* knowledge of where to place finer grids. Using grid clustering or grid enrichment techniques, they automatically allocate fine resolution to areas of interest. They are thus able to capture the physical and chemical processes that occur in the atmosphere much more efficiently than their fixed grid counterparts.

The adaptive grid methodology used here is based on the Dynamic Solution Adaptive Grid Algorithm (DSAGA) of Benson and McRae (1991), which was later extended for use in air quality modeling by Srivastava et al. (2000). It employs a structured grid with a constant number of grid nodes. The modeling domain is partitioned into  $N \times M$  quadrilateral grid cells. The grid nodes are re-positioned in a two-dimensional space throughout the simulation according to a weight function which represents the resolution requirements. The areas of the grid cells change due to grid node movements but the connectivity of the grid nodes remains the same. Further, since the number of grid nodes is fixed, refinement of grid scales in some regions is accompanied by coarsening in other regions where the weight function has smaller values. This results

---

\* Talat Odman, Georgia Institute of Technology, Atlanta, Georgia, 30332-0512, talat.odman@ce.gatech.edu, Telephone: 770-754-4971, Fax: 770-754-8266. Maudood Khan, Georgia Institute of Technology, Atlanta, Georgia, 30332-0512. Ravi Srivastava, U.S. Environmental Protection Agency, Research Triangle Park, North Carolina, 27711. Scott McRae, North Carolina State University, Raleigh, North Carolina, 27695-7910.

in optimal use of computational resources and yields a continuous multiscale grid where the scales change gradually. Unlike nested grids there are no grid interfaces, therefore, numerical problems related to the discontinuity of grid scales are avoided.

The adaptive grid algorithm was applied to problems with increasing complexity and relevance to air quality modeling. Starting with pure advection tests (Srivastava et al., 2000), it was applied to reactive flows (Srivastava et al., 2001a) and to the simulation of a power-plant plume (Srivastava et al., 2001b). In all these applications, the adaptive grid solution was more accurate than a fixed, uniform grid solution obtained by using the same number of grid nodes. To achieve the same level of accuracy with the fixed uniform grid required significantly more computational resources than the adaptive grid solution. In this paper, we describe how the adaptive grid algorithm was implemented in an urban-to-regional scale AQM. After a brief discussion of model components, we report preliminary results from the first application of the adaptive grid AQM.

## 2. METHODOLOGY

An adaptive grid AQM simulation has two fundamental steps: a grid adaptation step, that is responsible for repositioning of grid nodes according to the grid resolution requirements, and a solution step, that simulates the physical and chemical processes that occur in the atmosphere. The solution (i.e., concentration fields) remains unchanged during the adaptation step, and the weight function clusters the grid nodes in regions where finer resolution grids are required. In preparation for the solution step, the fields of meteorological inputs and emissions must be mapped onto the new grid locations. This task is also considered part of the adaptation step and is undertaken by efficient search and intersection algorithms. During the solution step, the grid nodes remain fixed while the solution is advanced in time. Ideally, the adaptation step should be repeated after each solution step owing to the change in resolution requirements. However, since the mapping of meteorological and emissions data is computationally expensive, we have chosen to apply the adaptation step less frequently. Whereas, the solution is advanced in time by 1 hour in several time steps, the adaptation step is performed once every hour. In order to ensure numerical stability, we require that the Courant number be smaller than unity while determining the time step of the solution. The rest of this section consists of a more detailed description of the adaptation and solution steps.

### 2.1. Adaptation Step

The key to adaptation is a weight function that determines where grid nodes need to be clustered for a more accurate solution. Such a weight function,  $w$ , can be built from a linear combination of the errors in the concentrations of various chemical species:

$$w \propto \sum_n \mathbf{a}_n \nabla^2 c_n \quad (1)$$

where  $\nabla^2$ , the Laplacian, represents the error in  $c_n$ , the computed value of the concentration of species  $n$ . The chemical mechanisms used in AQMs usually have a large number of species. Due to non-homogeneous distribution of emissions and disparate

residence times, each species may have very different resolution requirements. Determining  $\mathbf{a}_n$  such that pollutant concentrations (e.g., ozone) can be estimated most accurately is a current research topic. Here, all  $\mathbf{a}_n$  are set to zero, except the one for nitric oxide (NO). Further, the grid adaptation is restricted to the horizontal plane, and the same grid structure, which is determined by the surface layer NO concentrations, is used for all vertical layers. This, combined with the requirement that the Courant number should be less than unity, may result in very small solution time steps because of high wind speeds aloft. Adaptation in the vertical direction is possible but more complicated.

The grid nodes are repositioned by using the weight function. The new position of the grid node  $i$ ,  $\bar{P}_i^{new}$ , is calculated as:

$$\bar{P}_i^{new} = \frac{\sum_{k=1}^4 w_k \bar{P}_k}{\sum_{k=1}^4 w_k} \quad (2)$$

where  $\bar{P}_k$ ,  $k=1, \dots, 4$ , are the original positions of the centroids of the four cells that share the grid node  $i$ , and  $w_k$  is the weight function value associated with each centroid.

Once the grid nodes are repositioned, cell-averaged species concentrations must be recomputed for the adapted grid cells. Holding the concentration field fixed and moving the grid is numerically equivalent to simulating the advection process on a fixed grid. Therefore, we use a high-order accurate and monotonic advection scheme known as the piecewise parabolic method (Collela and Woodward, 1984) to interpolate concentrations from the old to the new grid locations.

The calculation of the weight function, the movement of the grid nodes, and the interpolation of species concentration from the old to the new grid locations are three distinct tasks of an iterative process. The process continues until the maximum grid node movement is less than a preset tolerance. A very small tolerance may lead to a large number of iterations. On the other hand, a large tolerance may not ensure adequate resolution of the solution field. Currently, we stop iterating when, for any grid node, the movement is less than 5% of the minimum distance between the node in question and the four nodes to which it is connected.

After the grid nodes are repositioned, emissions and meteorological data must be processed to generate the necessary inputs for the solution step. Note that, unlike the practice with fixed grid AQMs, this processing could not be performed prior to the simulation because there is no *a priori* knowledge of where the nodes would be located at any given time. In case of meteorological data, an ideal solution would be to run a meteorological model (MM), which can operate on the same adaptive grid, in parallel with the AQM. This would ensure dynamic consistency of meteorological inputs, but such a MM is currently nonexistent. Therefore, hourly meteorological data are obtained from a high-resolution, fixed-grid MM simulation and interpolated onto the adaptive grid. For mass conservation, as a minimum requirement, the vertical wind components are readjusted later during the solution step as described in Odman and Russell (2000).

The processing of emission data is computationally expensive, requiring identification of various emission sources in the adapted grid cells. Here, we treat all emission sources in two categories: point and area sources. For simplicity, the mobile sources have been included in the area-source category, but treating them as line sources

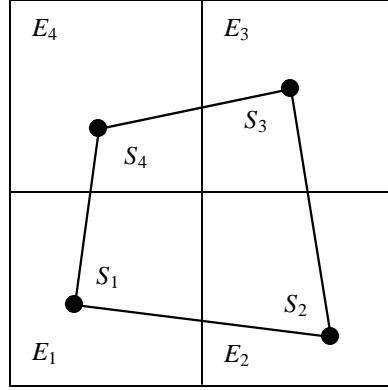


**Figure 1.** Intersection of an adapting grid cell with the area-source emissions grid.

would yield better resolution. For the point sources, the grid cell containing the location of each stack must be identified. The search may be quite expensive if there are thousands of stacks in the modeling domain. However, assuming that the cell containing the stack before adaptation would still be in close proximity of the stack after adaptation, the search can be localized. The localization of the search provides significant savings over more general, global searches. As for the area sources, they are first mapped onto a uniform high-resolution *emissions grid* using geographic information systems. This is done in order to avoid higher computational costs associated with processing of emissions from highly irregular geometric shapes presented by highways and counties. Around each adaptive grid cell there is a box of emissions grid cells  $E_i, i = 1, \dots, n$ , as illustrated in Figure 1. Once each  $E_i$  is identified, then their polygonal intersections with the adaptive grid cell are determined. Finally, the areas of these polygons,  $S_i$ , are multiplied by the emission fluxes of  $E_i$  and summed over  $n$  to yield the total mass emitted into the adaptive grid cell. This process is performed for all adaptive grid cells.

The final step in preparation for the solution step is reestablishing a uniform grid for easy computation of the solution. This requires computation of a transformation from the  $(x, y)$  space where the grid is non-uniform to the  $(\mathbf{x}, \mathbf{h})$  space where the grid would be uniform. The calculation of the Jacobian of the transformation and other necessary metrics (i.e.,  $\partial \mathbf{x} / \partial x, \partial \mathbf{x} / \partial y, \partial \mathbf{h} / \partial x, \partial \mathbf{h} / \partial y$ ) concludes the adaptation step.

## 2.2. Solution Step

The atmospheric diffusion equation in the  $(\mathbf{x}, \mathbf{h}, \mathbf{s})$  space can be written as

$$\begin{aligned} \frac{\partial(Jc_n)}{\partial t} + \frac{\partial(Jv^x c_n)}{\partial \mathbf{x}} + \frac{\partial(Jv^h c_n)}{\partial \mathbf{h}} + \frac{\partial(Jv^s c_n)}{\partial \mathbf{s}} + \frac{\partial}{\partial \mathbf{x}} \left( JK^{xx} \frac{\partial c_n}{\partial \mathbf{x}} \right) \\ + \frac{\partial}{\partial \mathbf{h}} \left( JK^{hh} \frac{\partial c_n}{\partial \mathbf{h}} \right) + \frac{\partial}{\partial \mathbf{s}} \left( JK^{ss} \frac{\partial c_n}{\partial \mathbf{s}} \right) = JR_n + JS_n \end{aligned} \quad (3)$$

where  $c_n$ ,  $R_n$ , and  $S_n$  are the concentration, chemical reaction, and emission terms of species  $n$ , respectively, and  $\mathbf{s}$  is a terrain-following vertical coordinate.  $J$  is the Jacobian of the coordinate transformation:

$$J = \frac{1}{m^2} \frac{\partial z}{\partial \mathbf{s}} \left( \frac{\partial x}{\partial \mathbf{x}} \frac{\partial y}{\partial \mathbf{h}} - \frac{\partial y}{\partial \mathbf{x}} \frac{\partial x}{\partial \mathbf{h}} \right) \quad (4)$$

where  $m$  is the scale factor of a conformal map projection in the horizontal. The components of the wind vector in  $\mathbf{x}$  and  $\mathbf{h}$  directions are  $v^x$  and  $v^h$ :

$$\begin{aligned} v^x &= m \frac{\partial \mathbf{x}}{\partial x} U + m \frac{\partial \mathbf{x}}{\partial y} V \\ v^h &= m \frac{\partial \mathbf{h}}{\partial x} U + m \frac{\partial \mathbf{h}}{\partial y} V \end{aligned} \quad (5)$$

where  $U$  and  $V$  are real horizontal wind velocities rotated in the map's coordinate directions. The turbulent diffusivity tensor is assumed to be diagonal, and its elements are  $K^{xx}$ ,  $K^{hh}$ , and  $K^{ss}$ .  $K^{ss}$  can be expressed in terms of the vertical diffusivity  $K^{zz}$  as:

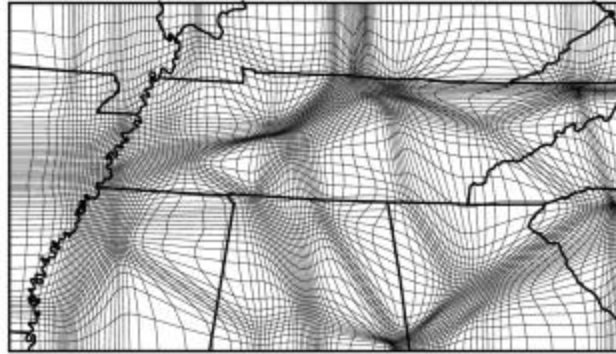
$$K^{ss} = \left( \frac{\partial \mathbf{s}}{\partial z} \right)^2 K^{zz}. \quad (6)$$

The expressions for  $v^s$  (the wind component in the  $\mathbf{s}$  direction),  $K^{xx}$ , and  $K^{hh}$  are omitted here due to space limitations. Since the grid is uniform in the  $(\mathbf{x}, \mathbf{h})$  space, solution algorithms can be taken directly from existing AQMs. We use those described by Odman and Ingram (1996).

### 3. MODEL VERIFICATION

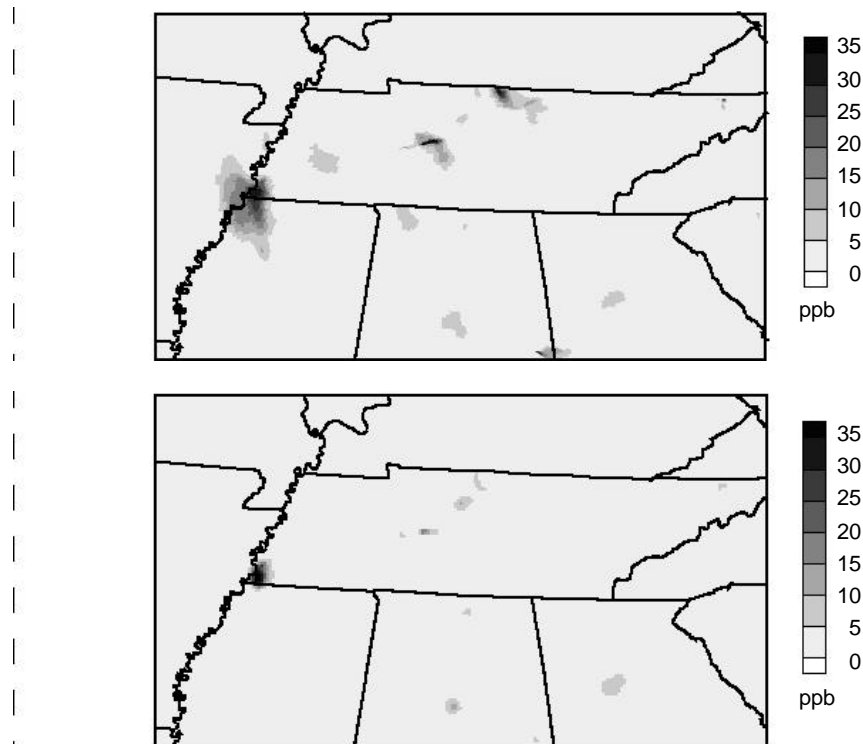
The adaptive grid AQM is being verified by simulating ozone air quality in the Tennessee Valley region for the July 7-17, 1995, period. Meteorological data from a  $4 \times 4$  km resolution simulation with the Regional Atmospheric Modeling System (RAMS) are being used. The emissions inputs for the region were developed from the Southern Appalachian Mountains Initiative (SAMI) inventory. There are over 9000 point sources in this domain including some of the largest power plants in the U.S.A. The area sources were mapped onto a  $4 \times 4$  km emissions grid. The AQM grid consists of 112 by 64 cells, initially at  $8 \times 8$  km resolution. In the vertical, there are 20 unequally spaced layers extending from the surface to 5340 m. Starting with 32 m, the thickness of each layer increases with altitude.

Figure 2 shows the grid at 7:00 EST on July 7. Since the adaptation step is performed once an hour, the grid shown will not change until 8:00 EST. Note that the grid size is reduced to few hundred meters around large point sources. With wind speeds larger



**Figure 2.** The grid used from 7:00 to 8:00 EST during the simulation of July 7, 1995.

than 10 m/s aloft, the solution time step can drop below 1 minute to keep the Courant number less than unity. Because of this, the simulation is progressing at the speed of about 2 hours of CPU time per simulation hour on a SUN Blade workstation (Model 1000)



**Figure 3.** NO concentrations at 7:00 EST on July 7, 1995, from adaptive grid (top) and 4x4 km fixed grid (bottom) AQM simulations.

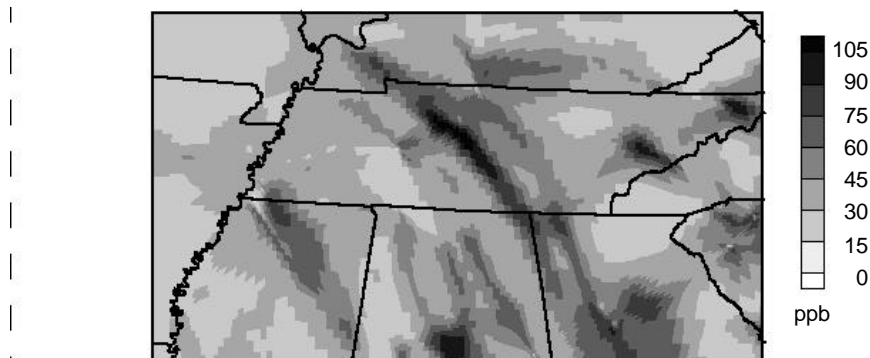


Figure 4. Ozone concentrations at 17:00 EST on July 7, 1995, from the adaptive grid AQM simulation.

with a 750 MHz Ultra SPARC III processor.

The surface layer NO concentrations at 7:00 EST that were used in generating the grid in Figure 2 are shown in Figure 3 (top frame). Also shown are the NO concentrations at the same hour from a  $4 \times 4$  km resolution fixed grid AQM simulation (bottom frame). The adaptive grid captures the NO gradients near source areas with a level of detail that is far superior to the fixed grid even though the latter used 4 times more grid nodes. Note that some large power plant stacks, such as Cumberland, are emitting above the stable boundary layer at this hour. Since their plumes do not affect the surface layer NO concentrations, no grid clustering is observed in Figure 2 around such stacks. During daytime hours, as such plumes mix down and start affecting the surface layer NO concentrations, grid nodes are clustered around them, along with other sources.

Figure 4 shows the ozone ( $O_3$ ) concentrations obtained from the adaptive grid AQM simulation at 17:00 EST on July 7, 1995. Since this is only the first day of the simulation, the  $O_3$  concentrations are probably still sensitive to the uniform initial conditions (35 ppb everywhere). However, the observed level of variability in the field and the captured detail in the gradients are encouraging. Once this simulation is finished,  $O_3$  fields will be compared to those obtained from fixed grid AQM simulation at  $4 \times 4$  and  $8 \times 8$  km resolutions using the same inputs and solution algorithms. To complete the verification, all simulated  $O_3$  fields will be compared to observations from routine monitoring network as well as intensive field studies conducted in the region during this episode.

#### 4. CONCLUSION

An adaptive grid, urban-to-regional scale AQM has been developed. A simulation with this model evolves as a sequence of adaptation and solution steps. During the adaptation step, the solution (i.e., concentration fields) is frozen in time. A weight function that can detect the error in the solution is used to move the nodes of a structured grid. Iterative movement of the grid nodes continues until the solution error is reduced sufficiently. During the solution step, the grid is held fixed and the solution is advanced in time. However, before this can be done, the meteorological and emissions inputs must be mapped onto the adapted grid. For meteorological inputs, data are interpolated from a

very-high-resolution mesoscale model simulation. For emissions, efficient search and intersection algorithms were developed to ensure proper allocation of point and area sources to the cells of the adapted grid. Using coordinate transformations, the non-uniform grid can be mapped into a space where it becomes uniform. The atmospheric diffusion equation in this new space has been derived. Since the form of the equation is very similar to forms in existing AQMs and the grid is uniform, numerical algorithms developed for fixed uniform grid AQMs can be used to advance the solution.

To verify the model, the July 7-17, 1995, ozone episode in the Tennessee Valley is being simulated. So far, the grid is adapting to dynamic changes in the NO fields as expected. Nodes are clustered around major emission sources with grid resolutions around 200 m. The NO and O<sub>3</sub> fields show gradients with a level of detail that is likely unprecedented for a regional simulation of this scale. However, the simulation is progressing slowly due to very short solution time steps. This will probably necessitate changes in solution algorithms such as using an implicit advection scheme that is not subject to the Courant stability limit. Adaptation criteria are also being developed that would consider the errors not only in NO but in other species as well, especially those involved in important O<sub>3</sub> formation reactions.

## 5. ACKNOWLEDGEMENTS

This research is supported by U.S. Environmental Protection Agency Grant No. R 827028-01-0. We thank Steve Mueller of the Tennessee Valley Authority for providing the meteorological data.

## 6. REFERENCES

- Benson, R. A., and McRae, D. S., 1991, A Solution adaptive mesh algorithm for dynamic/static refinement of two and three-dimensional grids, in: *Proceedings of the Third International Conference on Numerical Grid Generation in Computational Field Simulations*, Barcelona, Spain, p. 185.
- Collela, P., and Woodward, P. R., 1984, The piecewise parabolic method (PPM) for gas-dynamical simulations, *J. Comput. Phys.* **54**:174.
- Odman, M. T., and Russell, A.G., 1991, A multiscale finite element pollutant transport scheme for urban and regional modeling, *Atmos. Environ.* **25A**: 2385.
- Odman, M. T., and Ingram, C., 1996, *Multiscale Air Quality Simulation Platform (MAQSIP): Source Code Documentation and Validation*, MCNC Technical Report ENV-96TR002, Research Triangle Park, North Carolina, pp.11-32.
- Odman, M. T., Mathur, R., Alapaty, K., Srivastava, R. K., McRae, D. S., and Yamartino, R. J., 1997, Nested and adaptive grids for multiscale air quality modeling, in: *Next Generation Environmental Models and Computational Methods*, G. Delic, and M. F. Wheeler, eds., SIAM, Philadelphia, pp. 59-68.
- Odman, M. T., Russell, A. G., 2000. Mass conservative coupling of non-hydrostatic meteorological models with air quality models, in: *Air Pollution Modeling and its Application XIII*, S.-E.Gryning, and E. Batchvarova, eds., Kluwer Academic/Plenum Publishers, New York, pp. 651-660.
- Srivastava, R. K., McRae, D. S., and Odman, M. T., 2000, An adaptive grid algorithm for air quality modeling; *J. Comput. Phys.* **165**: 437.
- Srivastava, R. K., McRae, D. S., and Odman, M. T., 2001(a), Simulation of a reacting pollutant puff using an adaptive grid algorithm, *J. Geophys. Res.*, in press.
- Srivastava, R. K., McRae, D. S., and Odman, M. T., 2001(b), Simulation of dispersion of a power plant plume using an adaptive grid algorithm, *Atmos. Environ.*, in press.